arXiv:1406.7119v1 [cond-mat.mtrl-sci] 27 Jun 2014

Strain induced $\mathbb{Z}_2$ topological insulating state of β-As_2Te_3

Koushik Pal[1,2] and Umesh V. Waghmare[a)2]

[1)] *Chemistry and Physics of Materials Unit, Jawaharlal Nehru Centre for Advanced Scientific Research, Bangalore-560064, India*

[2)] *Theoretical Sciences Unit, Jawaharlal Nehru Centre for Advanced Scientific Research, Bangalore-560064, India*

Topological insulators are non-trivial quantum states of matter which exhibit a gap in the electronic structure of their bulk form, but a gapless metallic electronic spectrum at the surface. Here, we predict a uniaxial strain induced electronic topological transition (ETT) from a band to topological insulating state in the rhombohedral phase (space group: $R\bar{3}m$) of As_2Te_3 (β-As_2Te_3) through *first-principles* calculations including spin-orbit coupling within density functional theory. The ETT in β-As_2Te_3 is shown to occur at the uniaxial strain ϵ_{zz} = -0.05 (σ_{zz}=1.77 GPa), passing through a Weyl metallic state with a single Dirac cone in its electronic structure at the Γ point. We demonstrate the ETT through band inversion and reversal of parity of the top of the valence and bottom of the conduction bands leading to change in the $\mathbb{Z}_2$ topological invariant ν_0 from 0 to 1 across the transition. Based on its electronic structure and phonon dispersion, we propose ultra-thin films of As_2Te_3 to be promising for use in ultra-thin stress sensors, charge pumps and thermoelectrics.

[a)] Electronic mail:waghmare@jncasr.ac.in

Discovery of the non-trivial electronic topology in the layered semiconductors (Bi_2Se_3, Bi_2Te_3, Sb_2Te_3)[1,2] with tetradymite crystal structure (space group: R$\bar{3}$m, No: 166) have stimulated enormous research activity in exploration of exotic states like superconductivity, anomalous quantum Hall, and magneto-electric effects that have been predicted theoretically[3–5]. These materials, commonly known as topological insulators (TIs), are insulators in their bulk form, but exhibit a metallic electronic spectrum at their surfaces. The non-trivial topology of the bulk electronic states of Bi_2Te_3 type TI's arises from strong spin-orbit interactions[1]. The metallic state of the surface of a topological insulator is protected by the time reversal symmetry, and is robust against any non-magnetic perturbations. Berry phases of electronic states at the surface of a strong topological insulator prevent back scattering of electrons from impurities resulting in a dissipation-less conduction of current on its surface[6].

Arsenic telluride has a monoclinic structure with space group C2/m (α-As_2Te_3) at the ambient pressure, and has been investigated as a thermoelectric material in earlier works[7–10] showing that it has a lower thermoelectric figure of merit than Bi_2Te_3. There is room for improving the thermoelectric performance of As_2Te_3 by applying pressure or with epitaxial strain. The high pressure study of α-As_2Te_3 by Scheidemantel et el[10] revealed a pressure induced structural phase transition from monoclinic (α-As_2Te_3) to rhombohedral structure (β-As_2Te_3) near 7 GPa, leading to dramatic enhancement in its thermoelectric power. The β-As_2Te_3 phase can also be synthesized by rapid quenching from high temperature or by compressing monoclinic α-As_2Te_3 crystals[11–13].

The β-phase of As_2Te_3 is iso-structural to Bi_2Se_3 family of compounds with R$\bar{3}$m symmetry (space group No:166) having 5 atoms in the bulk unit cell. Electronic structure of β-As_2Te_3 has been determined within a non-relativistic description *i.e.* without including the spin-orbit coupling (SOC)[14], and it is found to be similar to that of Bi_2Te_3 (also determined without SOC)[14] with a direct band gap of 0.12 eV at the Γ point. As_2Te_3 contains a relatively light element *As* and hence relatively weaker SOC, which can however be tuned with strain or pressure modifying its electronic properties. For example, a number of materials belonging to different crystal symmetries (at ambiant conditions) have been predicted theoretically from the quantum materials repository by using a search model based on the strain-dependent electronic structure[15]. Motivated by this, we determine electronic structure of β-As_2Te_3 as a function of uniaxial strain along the c-axis including SOC, and show

that it undergoes a quantum phase transition on application of a modest uniaxial stress of $\sigma_{zz} = 1.77$ GPa to an interesting topological insulating state with a small gap, a property which can be exploited to make devices.

We use a combination of two different implementations of density functional theoretical (DFT) methods (a) the WIEN2K[16] code which is an all-electron full potential linearized augmented plane wave (FP-LAPW) based technique and (b) the QUANTUM ESPRESSO (QE)[17] code which treats only valence electrons replacing the potential of ionic core with a smooth pseudopotential. To obtain total energies and eigenvalues of the electrons in a solid using the FP-LAPW methods, we use a basis set achieved by dividing the unit cell into non-overlapping spherical regions centered at each atom and the interstitial region. Two different types of basis sets are used in these two regions. Plane wave basis set is used in the expansion of the electronic wave functions inside the interstitial region. It is augmented by atomic like wave functions (linear combination of the solutions of the radial Schrdinger equation and spherical harmonics) in the space inside every atomic sphere. These atomic-like wave functions form the basis set inside each non-overlapping atomic sphere. We use Perdew, Burke and Ernzerhof (PBE) parametrization[18] of the exchange-correlation energy functional derived with a generalized gradient approximation (GGA)[19]. Spin-orbit interaction has been included through a second variational procedure[20,21]. Truncation of the plane wave expansion of electronic wave functions inside the interstitial region is specified by a cut-off value of $R_{mt}{*}K_{max} = 7$, where R_{mt} is the radius of the smallest atomic sphere (muffin-tin), $K_{max} = 2.8$ a.u^{-1} is the plane wave cut-off vector, and charge density is Fourier expanded up to by $G_{max} = 12$ Ry$^{1/2}$, where G_{max} represents the maximum value of G vector in the Fourier expansion. We adopt the tetrahedron method for sampling integrations over the Brillouin zone with a $9 \times 9 \times 9$ uniform mesh of k-vectors.

Lattice-dynamical properties are determined within the framework of self-consistent density functional perturbation theory (DFPT) as implemented within the QE code[22]. Since the effect of SOC is negligible on phonon frequencies and character of the vibrational modes is unchanged without the SOC, we determine vibrational frequencies of β-As_2Te_3 within a non-relativistic description. We use norm-conserving pseudopotentials and plane wave basis truncated with cut-off energies of 60 Ry and 240 Ry in representing of wave functions and charge density respectively. In order to calculate the phonon dispersion, force constant matrices are obtained on a $2{\times}2{\times}2$ q-point mesh. The dynamical matrices at arbitrary wave

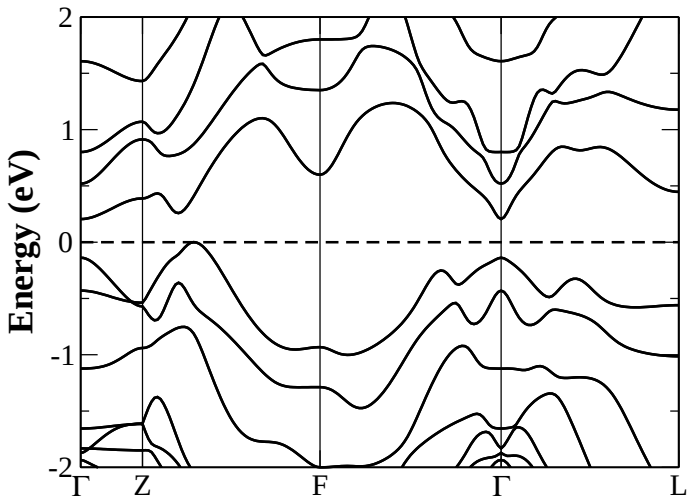

FIG. 1. Electronic structure of β-As_2Te_3 (space group: R$\bar{3}m$) at vanishing strain. Spin-orbit coupling is included in the electronic structure calculation. The overall product of parities of the occupied bands is positive which signifies that it is a band insulator when $\epsilon_{zz} = 0$.

vectors are then obtained using Fourier interpolations.

Lattice parameters of β-As_2Te_3 are taken from the Materials Project repository[23] with a_{hex}=4.089 $\mathring{A}$ and c_{hex}= 30.306 $\mathring{A}$. We keep a_{hex} fixed and apply uniaxial strain along the c-axis, relaxing the atomic positions at each value of the uniaxial strain until the forces on atoms become less that 1 mRy/bohr. In contrast to the earlier all-electron calculation[14], we include the SOC in determining electronic structure of β-As_2Te_3 as a function of ϵ_{zz}. From the electronic structure of β-As_2Te_3 (see Fig. 1) at vanishing strain, it is clear that the valence band maxima and the conduction band minima are located at points along different directions in the Brillouin zone (i.e. band gap is indirect). However, the direct band gap at Γ point is 0.35 eV, higher than the earlier estimate (0.12 eV), obtained without the SOC[14].

Electronic states near the Fermi level of β-As_2Te_3 are contributed largely by the p-orbitals of As and Te atoms. In Bi_2Se_3-type layered materials, compressive strain (ϵ_{zz}) was found to tune the strength of the SOC by reducing the inter quintuple-layer distance[24,25]. As β-As_2Te_3 shares similar layered crystal structure, ϵ_{zz} is expected to alter the strength of SOC and crystal field of β-As_2Te_3. At the compressive strain of ϵ_{zz} = -0.05, it exhibits a Weyl metallic state (see Fig. 2b), where a Dirac cone with linear dispersion (in 3-D) of the electronic bands appears at the Γ point. Upon further compression of the crystal along c-axis, repulsion between the electronic bands due to a strong SOC leads to reopening of

the bulk band gap, accompanied by the inversion of the top of the valence and bottom of the conduction bands at the Γ point. Naturally, parities of the bands also change their sign through the band inversion. Band inversion and parity reversal of bulk electronic bands are characteristics of an electronic topological phase transition which has been observed in Bi_2Se_3 (a strong $\mathbb{Z}_2$ topological insulator) as a function of strain with $\epsilon_{zz} = 0.06$ being its critical value[25]. Here, we show that β-As_2Te_3 undergoes an electronic topological transition at the ϵ_{zz}= -0.05, with a uniaxial stress $\sigma_{zz} = 1.77$ GPa.

We now determine the $\mathbb{Z}_2$ topological invariant quantity ν_0 of β-As_2Te_3 below and above the critical value of the strain using the technique of Fu and Kane[26] that equates the product of parities of states in the valence band manifold (see Table I) to $(-1)^{\nu_0}$. We find that the ν_0 is 0 and 1 for $\epsilon_{zz} >$ -0.05 and $\epsilon_{zz} <$ -0.05 (the critical strain ϵ_{zz}= -0.05) respectively, signifying that β-As_2Te_3 becomes a strong $\mathbb{Z}_2$ topological insulator for $\epsilon_{zz} <$ -0.05. Similar to Bi_2Se_3, Bi_2Te_3 and Sb_2Te_3 which are strong $\mathbb{Z}_2$ topological insulators at the ambient pressure[1], the top of valence and the bottom of conduction bands of β-As_2Te_3 have even and odd parities respectively in its topological insulating phase.

As shown in Fig. 2d, the band gap at the Γ point increases with strain beyond the transition point ($\epsilon_{zz} <$ -0.05), which is expected of a topological insulator, but with higher value of compressive strain (*e.g.* at $\epsilon_{zz} \sim$ -0.06), there is anti-crossing (see Fig. 2c & Fig. 3a) of these bands along the Γ-Z direction. This anti-crossing behavior can be explained with group theoretical analysis of their symmetries (see the next paragraphs). While the top-most valence band touches the Fermi level along Z-F direction, As_2Te_3 remains semiconducting at all $\epsilon_{zz} \neq$ -0.06, as evident in the electronic density of states (e-DOS) in Fig. 3b.

β-As_2Te_3 has both spatial inversion and time reversal symmetries. Inversion centre in the crystal ensures the degeneracy of the electronic bands at **k** and **-k** i.e. $\varepsilon_{n\alpha}(\mathbf{k}) = \varepsilon_{n\alpha}(\mathbf{-k})$, where $\varepsilon_{n\alpha}(\mathbf{k})$ represents the electron energy for the n-th band with spin index α at **k** wave vector in the Brillouin zone. On the other hand, the time reversal symmetry implies $\varepsilon_{n\alpha}(\mathbf{k}) = \varepsilon_{n\bar{\alpha}}(\mathbf{-k})$, where $\bar{\alpha}$ represents the spin opposite to α. When both symmetries are present, $\varepsilon_{n\alpha}(\mathbf{k}) = \varepsilon_{n\bar{\alpha}}(\mathbf{k})$, *i.e.* electronic bands acquire Kramers' double degeneracy at each **k** vector. As each electronic band in a $\mathbb{Z}_2$ topological insulator is doubly degenerate, the irreducible representation for each band is two dimensional (*i.e.* *E*, according to Mulliken's symbol). In the Hamiltonian with SOC, the point group at any **k** vector is a double group due to inclusion of time reversal symmetry. The irreducible representations of bands are hence determined

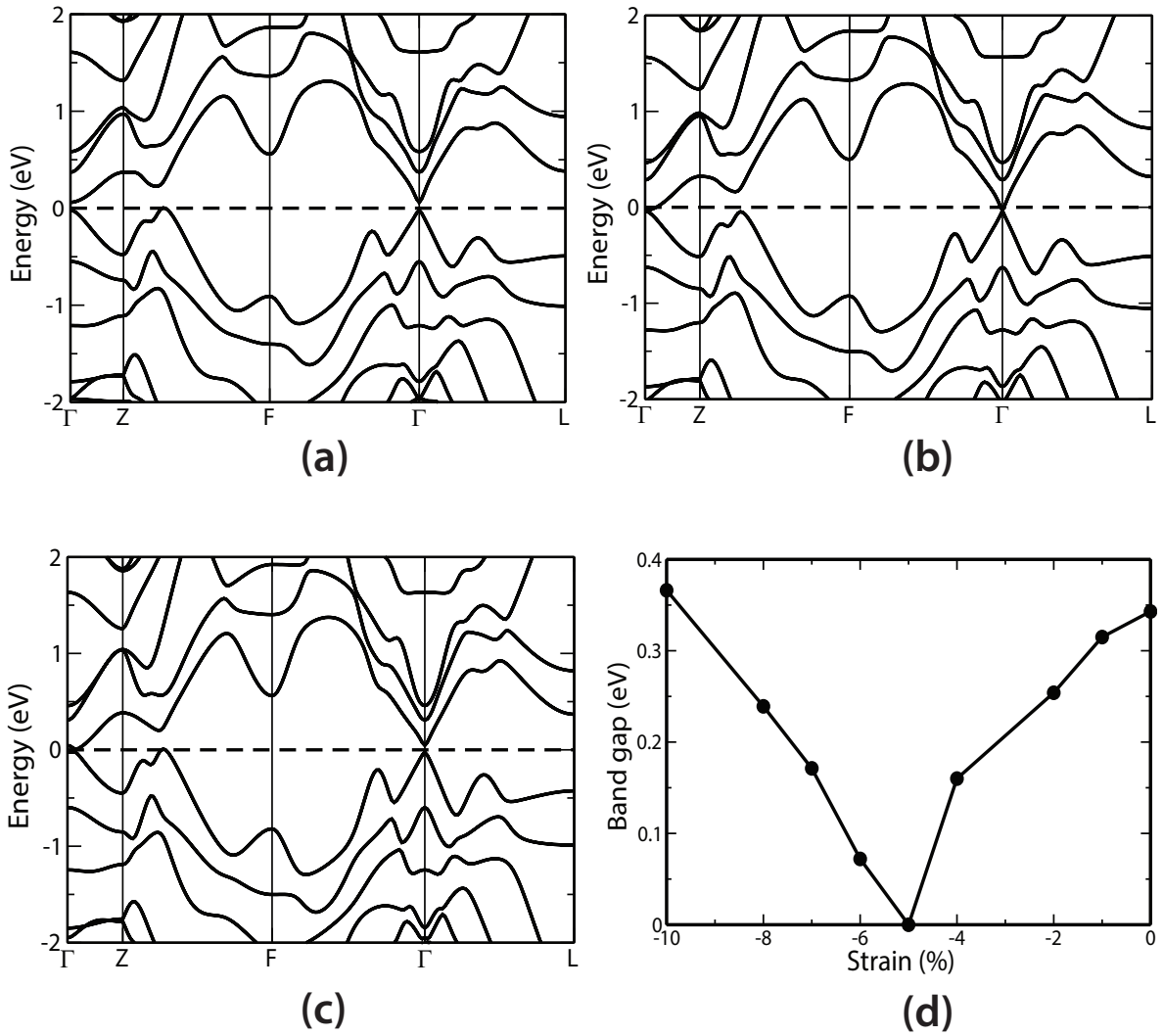

FIG. 2. Evolution of electronic bands and bulk band gap of β-As_2Te_3 as a function of uniaxial strain ϵ_{zz}. Electronic structures of bulk β-As_2Te_3 when the uniaxial strain are (a) ϵ_{zz}= -0.04, (b) ϵ_{zz}= -0.05, and (c) ϵ_{zz}= -0.06 showing the closing and reopening of the bulk band gap at the Γ point as a function of ϵ_{zz}. (d) Variation of the direct band gap at the Γ point as a function of uniaxial strain ϵ_{zz}. The electronic topological transition in β-As_2Te_3 passes through a metallic state at ϵ_{zz} = -0.05, where a linearly dispersing Dirac cone appears at the Γ point. The closing and reopening of the bulk band gap is accompanied with band inversion and parity reversal of states near the Fermi level. All the electronic structure calculations are performed taking spin-orbit coupling into account.

by the character table of the corresponding double group of a spin-orbit coupled system[27]. At Γ point (*i.e.* null **k** vector) in the Brillouin zone, the group of the k-vector is D_{3d}, and

electronic bands are labeled with representations (also known as small representations) of the double group of D_{3d}. The top of the valence and bottom of conduction bands in the topological insulating state have $E_{1/2g}(=\Gamma_{4+})$ and $E_{1/2u}(=\Gamma_{4-})$ symmetries respectively (see Fig. 3a, where the scale of electronic structure has been zoomed along the Γ-Z direction) at Γ. For **k** along z-direction (Γ-Z), the group of **k** lacks the inversion symmetry, and therefore its subgroup is C_{3v}, and bands along Γ-Z direction are labeled with irreducible representations of the double group of C_{3v}.

When two bands belong to the same irreducible representation, a coupling between them is allowed by symmetry. As a result, they avoid crossing each other and lead to an "anti-crossing"[28]. Electronic bands just above and below the Fermi level along the Γ-Z direction anti-cross each other, because they belong to the same irreducible representation ($E_{1/2}=\Gamma_4$) of C_{3v}. This analysis establishes that there can be no band crossing and closure of gap along Γ-Z direction, and hence the electronic structure (see DOS in Fig. 3b) of β-As_2Te_3 remains semiconducting as a function of ϵ_{zz} (including ϵ_{zz}=-0.06).

As the bandgap vanishes at the electronic topological transition in β-As_2Te_3, we expect a breakdown of the adiabatic approximation in the vicinity of the critical point. This broken adiabaticity would lead to Raman anomalies in a narrow range of stress near P_c through a strong coupling between the electrons and phonons near the transition[29]. Thus, it is of fundamental importance to measure the electronic and vibrational spectra of β-As_2Te_3 as a function of uniaxial strain, and confirm the presence of electronic topological transition and associated spectroscopic anomalies in β-As_2Te_3.

Since topological insulators typically exhibit good thermoelectric properties[30,31], we expect β-As_2Te_3 to be a better thermoelectric than its ambient pressure monoclinic phase, consistent with the finding of Ref. [10]. Thin films of topological insulators like Bi_2Te_3, Bi_2Se_3 are better thermoelectric materials[30] than their bulk counterpart due to the high mobility of the electrons on the metallic surface and low lattice thermal conductivity[31]. Strain engineering of thin films of Bi_2Se_3 was shown to be an effective way to optimize its thermoelectric figure of merit (ZT)[32], given by $ZT = \frac{\sigma S^2 T}{\kappa}$, where σ, S and, κ are electrical conductivity, Seebeck coefficient and thermal conductivity respectively.

Low κ is key to thermoelectric performance of a material. As acoustic phonon bands of β-As_2Te_3 are limited to range of frequencies less than 50 cm^{-1} (see Fig. 4), and κ depends quadratically on slope of the acoustic band, we expect a rather low thermal conductivity of

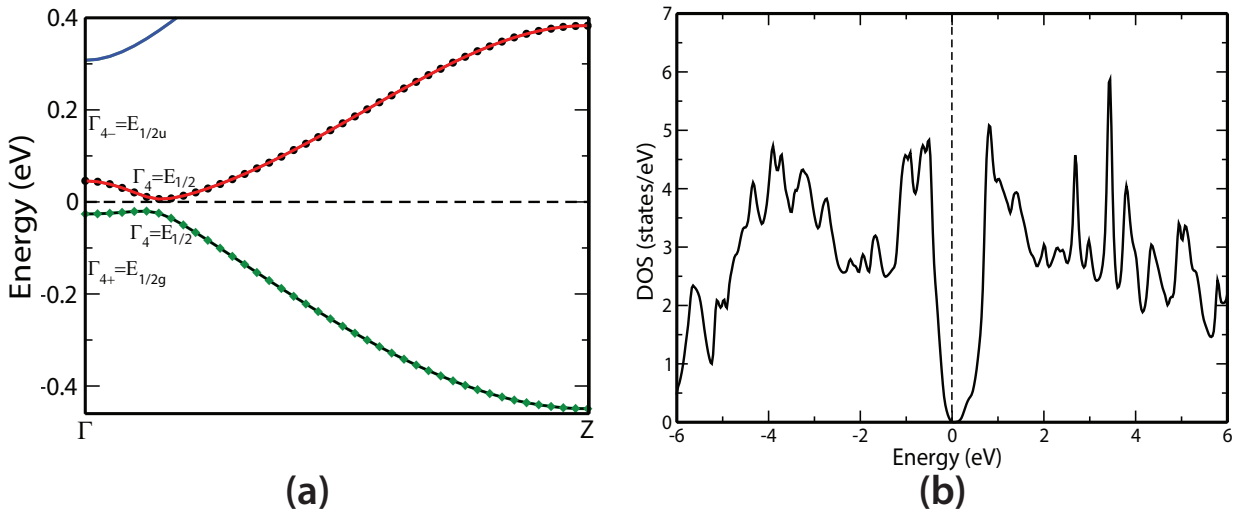

FIG. 3. (a) Electronic structure of β-As_2Te_3 at ϵ_{zz}= -0.06 with spin-orbit coupling zoomed along the Γ-Z direction. The electronic states near the Fermi level having the same irreducible representations lead to an anti-crossing situation as discussed in the text. (b) The total electronic density of states (DOS) of β-As_2Te_3 at ϵ_{zz}= -0.06 show semiconducting nature of the material in its topological insulating state.

β-As_2Te_3 in all the three directions. The narrow gap of β-As_2Te_3 will facilitate high electrical conductivity at room temperature, and the asymmetry in its DOS (Fig. 3b) across the gap is expected to yield a high S (e.g. at ϵ_{zz} = -0.06, band gap is 0.06 eV). Since its narrow band-gap and the symmetry of its frontier states are sensitive to uniaxial stress, β-As_2Te_3 has the promise of a good thermoelectric whose properties are tunable with stress field.

With frequencies of all its phonons less than 200 cm^{-1}, vibrational entropy gives greater stability to β-As_2Te_3 with increasing temperature. As the quintuple layers of β-As_2Te_3 are held together by the weak van der Waals forces, it can be readily prepared in the form of an ultra-thin film. Surface of a topological insulator exhibits a robust two dimensional electron gas (2DEG) with a high carrier mobility, while that of a band insulator shows none. This property can be used to create a charge pump based on As_2Te_3 that is driven by mechanical stress field.

In conclusion, we predict a uniaxial strain induced transition from band to topological insulating state in β-As_2Te_3 using *first-principles* density functional theory based calculations, highlighting the importance of spin-orbit coupling. It exhibits a direct band gap of 0.35 eV at the Γ point at ambient conditions, and passes through a Weyl metallic state with linearly

ϵ_{zz} = -0.04	+ - + - + + - + - - + - - - ; +	(+)
ϵ_{zz} = -0.06	+ - + - + + - + - - + - - + ; -	(-)

TABLE I. Parities of the fourteen occupied bands below the Fermi level and the lowest unoccupied band above the Fermi level across the transition point (ϵ_{zz} = -0.05) for β-As_2Te_3. The Product of parities of the valence band manifold are given in the rightmost column and are indicated within the brackets. Positive and negative signs within the brackets mean that for $\epsilon_{zz} >$ -0.05, β-As_2Te_3 is a band insulator which undergoes a quantum phase transition and becomes a topological insulator upon increasing the strain beyond it.

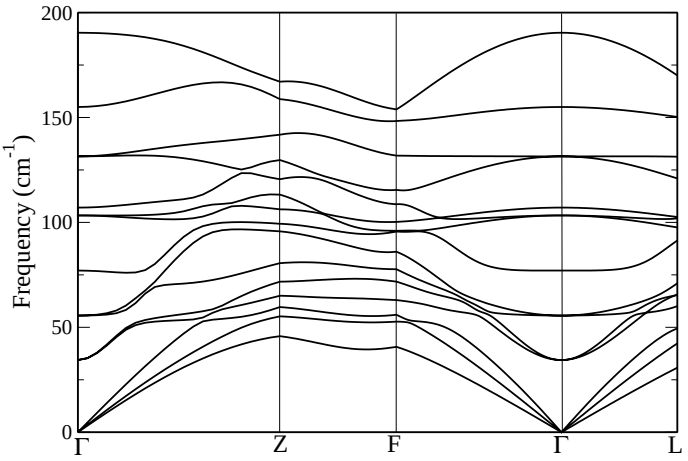

FIG. 4. Phonon dispersion of β-As_2Te_3 at ϵ_{zz}= -0.06 calculated within a non-relativistic description.

dispersing bands typical of a Dirac cone at ϵ_{zz} = -0.05 with non-zero gaps on the two sides of the transition. The ETT in the rhombohedral phase of As_2Te_3 has been demonstrated through the band inversion and parity reversal of the top of the valence and bottom of conduction bands across the critical strain, accompanied by a change in the $\mathbb{Z}_2$ topological invariant. Finally, uniaxial stress can be used to tune electronic gap and thermoelectric performance of thin films of β-As_2Te_3, which augurs well for its applications.

UVW thanks funding from a JC Bose National Fellowship of the Department of Science and Technology of Govt of India. KP thanks JNCASR for a fellowship and acknowledge the computational resources from TUE-CMS, JNCASR.

REFERENCES

[1]H. Zhang, C. X. Liu, X. L. Qi, X. Dai, Z. Fang and S. C. Zhang, Nature Physics **5**, 438 (2009).

[2]D. Hsieh, Y. Xia, D. Qian, L. Wray, F. Meier, J. H. Dil, J. Osterwalder, L. Patthey, A. V. Fedorov, H. Lin, A. Bansil, D. Grauer, Y. S. Hor, R. J. Cava, and M. Z. Hasan, Phys. Rev. Lett. **103**, 146401 (2009b).

[3]L. Fu, and C. L. Kane, Phys. Rev. Lett. **100**, 096407 (2008).

[4]A. Essin, J. E. Moore, D. Vanderbilt, Phys. Rev. Lett. **102**, 146805 (2009).

[5]A. Essin, A. M. Turner, J. E. Moore, and D. Vanderbilt, Phys. Rev. B **81**, 205104 (2010).

[6]M. Z. Hasan and C. Kane, Rev. Mod. Phys. **82**, 3045 (2010).

[7]T. C. Harman, B. Paris, S. E. Miller, L. Goering, J. Phys. Chem. Solids, **2**, 181 (1957).

[8]J. Black, E. M. Vonwell, L. Seigle, C. W. Spencer, J. Phys. Chem. Solids, **2**, 240 (1957).

[9]E. I. Yarembash, E. S. Vigileva, J. Russian, J. INorg. Chem. **7**, 1437 (1962).

[10]T. J. Scheidemantel, J. F. Meng, and J. V. Badding, J. Phys. Chem. Solids, **66**, 1744 (2005).

[11]S. Toscani, J. Dugue, R. Ollitrault, and R, Ceolin, Theor. Chim. Acta, **186**, 247 (1991).

[12]V. A. Kirkinskii, V. G. Yakushev, Inorg. Mater. (USSR) **10**, 1431 (1974).

[13]V. A. Yakushev, V. A. Kirkinskii, D. Akad, Nauk SSSR **186**, 882 (1969).

[14]T. J. Scheidemantel, V. Badding, Solid Stat Commun. **127** 667 (2003).

[15]K. Yang, W. Setyawan, S. Wang, M. Buongiorno Nardelli, and S. Curtarolo, Nature Materials **11** 614 (2012).

[16]P. Blaha, K. Schwarz, G. K. H. Madsen, D. Kvasnicka and J. Luitz, WIEN2k, An Augmented Plane Wave Local Orbitals Program for Calculating Crystal Properties (K 2001. ISBN 3-9501031-1-2.

[17]Quantum-ESPRESSO is a community project for high-quality quantum-simulation software, based on density-functional theory, and coordinated by P. Giannozzi. See `http://www.quantum-espresso.org` and `http://www.pwscf.org`.

[18]J. P. Perdew, K. Burke, M. Ernzerhof, Phys. Rev. Lett. **77**, 3865 (1996).

[19]X. Hua, X. Chen, W. A. Goddard III, Phys. Rev. B **55**, 16103 (1997).

[20]A. H. MacDonald, W. E. Pickett, and D. D. Koelling, J. Phys. C **13**, 2675 (1980).

[21]P. Novak, F. Boucher, P. Gressier, P. Blaha, and K. Schwarz, Phys. Rev. B **63**, 235114

(2001).

[22]S. Baroni, S. de Gironcoli, A. Dal. Corso, and P. Gianozzi, Rev. Mod. Phys. **73**, 515 (2000).

[23]A. Jain, S.P. Ong, G. Hautier, W. Chen, W.D. Richards, S. Dacek, S. Cholia, D. Gunter, D. Skinner, G. Ceder, App. Phys. Lett. Mat. **1**, 011002 (2013).

[24]S. M. Young, S. Chowdhury, E. J. Walter, E. J. Mele, C. L. Kane, and Andrew M. Rappe, Phys. Rev. B **84** 085106 (2011).

[25]W. Liu, X. Peng, C. Tang, L. Sun, K. Zhang, J. Zhong, Phys. Rev. B **84**, 245105 (2010).

[26]L. Fu, and C. L. Kane, Phys. Rev. B **76**, 045302 (2007).

[27]M. Dresselhaus, G. Dresselhaus, and A. Jorio, Group Theory: Application to the Physics of Condensed Matter, Springer (2008).

[28]M. Endo, S. Iijima, M. S. Dresselhaus, Carbon Nanotubes, Pergamon, ISBN:008 0426824, Elsevier Science Limited (1996).

[29]A. Bera, K. Pal, D. V. S. Muthu, S. Sen, P. Guptasarma, U. V. Waghmare and A. K. Sood, Phys. Rev. Lett. **110**, 107401 (2013).

[30]P. Ghaemi, R. S. K. Mong, and J. E. Moore, Phys. Rev. Lett. **105**, 166603 (2010).

[31]Z. Fan, J. Zheng, H.-Q. Wang, and J.-C. Zheng, Nanoscale Res. Lett. **7**, 570 (2012).

[32]Y. Saeed, N. Singh, and U. Schwingenschlogl, App. Phys. Lett. **104**, 033105 (2014).